




Body composition profiling at 0.55T: Feasibility and precision

Krishna S. Nayak¹  | Sophia X. Cui²  | Bilal Tasdelen¹ | Ecrin Yagiz¹ | Sarah Weston³ | Xiaodong Zhong²  | André Ahlgren³

¹Electrical and Computer Engineering, University of Southern California, Los Angeles, California, USA

²Siemens Medical Solutions USA, Los Angeles, California, USA

³AMRA Medical, Linköping, Sweden

Correspondence

Krishna S. Nayak, 3740 McClintock Ave, Suite 400C, Los Angeles, CA 90089-2564, USA.

Email: knayak@usc.edu

Funding information

National Science Foundation, Grant/Award Number: 1828736

Purpose: Body composition MRI captures the distribution of fat and lean tissues throughout the body, and provides valuable biomarkers of obesity, metabolic disease, and muscle disorders, as well as risk assessment. Highly reproducible protocols have been developed for 1.5T and 3T MRI. The purpose of this work was to demonstrate the feasibility and test-retest repeatability of MRI body composition profiling on a 0.55T whole-body system.

Methods: Healthy adult volunteers were scanned on a whole-body 0.55T MRI system using the integrated body RF coil. Experiments were performed to refine parameter settings such as TEs, resolution, flip angle, bandwidth, acceleration, and oversampling factors. The final protocol was evaluated using a test-retest study with subject removal and replacement in 10 adult volunteers (5 M/5F, age 25–60, body mass index 20–30).

Results: Compared to 1.5T and 3T, the optimal flip angle at 0.55T was higher (15°), due to the shorter T1 times, and the optimal echo spacing was larger, due to smaller chemical shift between water and fat. Overall image quality was comparable to conventional field strengths, with no significant issues with fat/water swapping or inadequate SNR. Repeatability coefficient of visceral fat, subcutaneous fat, total thigh muscle volume, muscle fat infiltration, and liver fat were 11.8 cL (2.2%), 46.9 cL (1.9%), 14.6 cL (0.5%), 0.1 pp (2%), and 0.2 pp (5%), respectively (coefficient of variation in parenthesis).

Conclusions: We demonstrate that 0.55T body composition MRI is feasible and present optimized scan parameters. The resulting images provide satisfactory quality for automated post-processing and produce repeatable results.

KEYWORDS

0.55 tesla, body composition MRI, low field, metabolic disease, obesity, screening

A preliminary version of this work was presented at the 2022 ISMRM Workshop on Low Field MRI, Abstract #41.

This is an open access article under the terms of the [Creative Commons Attribution-NonCommercial](https://creativecommons.org/licenses/by-nc/4.0/) License, which permits use, distribution and reproduction in any medium, provided the original work is properly cited and is not used for commercial purposes.

© 2023 The Authors. *Magnetic Resonance in Medicine* published by Wiley Periodicals LLC on behalf of International Society for Magnetic Resonance in Medicine.

1 | INTRODUCTION

Body composition MRI captures the distribution of fat and lean tissues throughout the human body, and provides valuable biomarkers of obesity, metabolic disease, and muscle disorders. Its importance is underscored by the inclusion in large population and longitudinal studies such as the UK Biobank and Dallas Heart Study.^{1,2} Especially MRI-based body composition is intriguing since it can yield high-precision measurements and measure body composition metrics not available with modalities such as bioelectrical impedance analysis, dual X-ray absorptiometry, or CT. Protocols have been optimized for 1.5T and 3T field strengths previously, and both accuracy and reproducibility are well-established.³

MRI-based body composition uses chemical shift encoded MRI which exploits the resonance phase-shift between fat and water to calculate fat and water only images from a single acquisition. The two-point Dixon MRI is the most time efficient chemical shift encoded technique acquiring only two echoes,⁴ and when applied to a 3D-spoiled gradient-recalled echo readout (e.g., VIBE) it allows for rapid chemical shift encoded imaging with acceptable breath holds and scan time. Multiple overlapping stations are acquired to produce continuous whole-body coverage. To obtain body composition measurements from the acquired 3D images requires post-processing in terms of image calibration, segmentation, and measurement algorithms. Calibration of the fat image can be achieved using the fat-referenced MRI technique, which uses the adipose tissue as an inherent reference to produce a quantitative fat concentration image.^{5,6} Once calibrated, the images are segmented into individual compartments and body composition metrics are calculated. Common MRI-based body composition metrics are visceral adipose tissue (VAT) volume, abdominal subcutaneous adipose tissue (ASAT) volume, thigh muscle volume, thigh muscle fat infiltration (MFI), and liver fat. Since fat-referenced MRI yields fat concentration images, the metrics account for partial volume effects, in contrast to conventional binary segmentation.³ The multi-echo Dixon technique is commonly used to quantitatively assess proton density fat fraction (PDFF).⁷ This sequence is typically acquired with six echoes and is available on all major MRI platforms.

Recently, there has been substantial interest in whole-body low field systems,^{8,9} due in part to the opportunity for reduced system cost, opportunity for a wider bore, reduced acoustic noise, better safety profile (specific absorption rate, etc.), and reduced artifact around metallic implants.¹⁰ The lower system cost could make MRI viable in new settings, and for screening applications including body composition. The opportunity for wider

bore is also favorable for studies of obesity and its associated adverse health outcomes. Low-field MRI also faces unique challenges including lower SNR due to reduced polarization, increased concomitant field effects,^{11,12} and reduced chemical shift requiring larger echo spacing for Dixon-based techniques.^{4,13}

In this work, we develop and evaluate a 0.55T body composition profile MRI protocol paired with automated post-processing. We adapt a 1.5T protocol that is in widespread use and re-optimize its parameters for the 0.55T field strength. We evaluate test-retest repeatability of the final protocol and performance of automated post-processing.

2 | METHODS

Neck-to-knee MRI scans were performed using a whole-body 0.55T system (prototype MAGNETOM Aera XQ, Siemens Healthcare, Erlangen, Germany). The hardware modifications have been described previously.¹⁰ Briefly, a state-of-the-art 1.5T commercial MRI system was ramped down to 0.55T and fitted with modified components to image ¹H at the 23.6 MHz resonant frequency. Ten healthy adult volunteers were scanned under a protocol approved by our Institutional Review Board, after providing written informed consent. The neck-to-knee coverage was realized using six overlapping 2-point Dixon sequences with preset table locations (i.e., no manual planning) and using the integrated body RF coil. Further MRI parameters are listed in Table 1. The liver was scanned employing conventional multi-channel receive only surface coils using the 6-point Dixon sequence (LiverLab) with factory default parameters from 1.5T (referred to as 'liver PDFF 6p'),¹⁴ as well as a multi-echo GRE sequence for liver T2* measurement. The liver T2* measurement was used for post-hoc T2* correction of an alternative liver PDFF measurement extracted from the fat-referenced 2-point Dixon data (referred to as 'liver PDFF 2p') this method has been previously described and validated.³

2.1 | Protocol optimization

Experiments were performed to iteratively refine parameter settings such as flip angle (FA), TEs, resolution, bandwidth, partial-Fourier, and slice oversampling factors. Measured tissue signal as a function of FA was compared against Bloch simulations. During TE selection, we used the minimum TE as the first approximate in-phase echo, in order to keep the TR and overall scan times short. This is different from 1.5T and 3T protocols which have greater flexibility due to the larger chemical shift. We explored

TABLE 1 Abbreviated listing of optimized parameters for 0.55T MRI body composition profiling

Parameter	2-point Dixon (breath-hold)	2-point Dixon (thighs)
TE (ms)	2.45 (min)/6.47 (OP)	2.54 (min)/6.47 (OP)
TR (ms)	9.48 (min)	9.53 (min)
FOV (mm)	500	500
Slice thickness (mm)	5	5
Readout bandwidth (Hz/Px)	250	250
Base resolution	128	192
Phase oversampling	0%	75%
Slice oversampling	18%	17%
Slices per slab	44	48
Phase resolution	75%	75%
Slice resolution	100%	100%
Phase partial Fourier	6/8	Off
Slice partial Fourier	5/8	Off
Table positions (landmark manubrium)	F30 F200 F370	F550 F730 F900
Resp. control	Breath-hold	Off

Note: Full details are provided in Table S1.

Abbreviation: FOV = field of view, OP = out-of-phase, TE = echo time, TR = repetition time.

several spatial resolutions with the finest matching 1.5T. Receiver bandwidth was made as low as possible for the given echo spacing, namely 250 Hz/Px, in order to maximize SNR. The fat-water frequency difference at 0.55T is approximately 80 Hz. A 250 Hz/Px readout bandwidth at 0.55T results in a fat chemical shift of approximately 0.3 pixels or 1.3 mm. This is comparable to the readout bandwidth choice of around 500 Hz/Px at 1.5T, which has a fat-water frequency difference of approximately 220 Hz and therefore a fat chemical shift of approximately 0.4 pixels or 1.5 mm. Partial-Fourier and slice oversampling factors were also tested among the range commonly used in other MRI applications, 62.5% to 100% and 0% to 50%, respectively.

2.2 | Prospective study

The optimized protocol was evaluated in 10 adult subjects. Each subject was scanned twice with a 5- to 10-min break in between during which the subject was removed from the scanner. The overall protocol took ~30 min including all breaks. The MR images were analyzed with the cloud-based service AMRA Researcher (AMRA Medical, Linköping, Sweden). Briefly, the post-processing includes the following steps: (1) calibration of fat images using fat-referenced MRI, (2) registration of atlases with ground truth labels for fat and muscle compartments to the acquired MRI dataset to produce automatic

segmentations, (3) quality control by two independent trained operators including the possibility to adjust and approve the final segmentations, and (4) quantification of fat volumes, muscle volumes, and MFI within the segmented regions. For liver PDFF, nine regions of interest are manually placed, evenly distributed in the liver volume, while avoiding major vessels and bile ducts.

The following body composition profile measurements were calculated from each scan: VAT, ASAT, left/right anterior/posterior thigh muscle volume and MFI, total thigh muscle volume, mean anterior thigh MFI, liver PDFF (6p) and liver PDFF (2p).

2.3 | Evaluation

The operator quality control in AMRA Researcher includes grading the signal quality in each of the segmented regions on a three-level scale according to: (1) good signal quality, (2) minor signal quality issue (still measurable), and (3) major signal quality issue (not possible to produce any meaningful measurement). The test-retest repeatability (precision) was calculated as the within-subject standard deviation (s_w) using one-way analysis of variance with the subject ID as the independent variable. The repeatability coefficient was calculated as $1.96 \times \sqrt{2} \times s_w$. Within-subject coefficient of variation (CV_w) was estimated by calculating all subject-wise coefficients of variation and then taking the root mean square

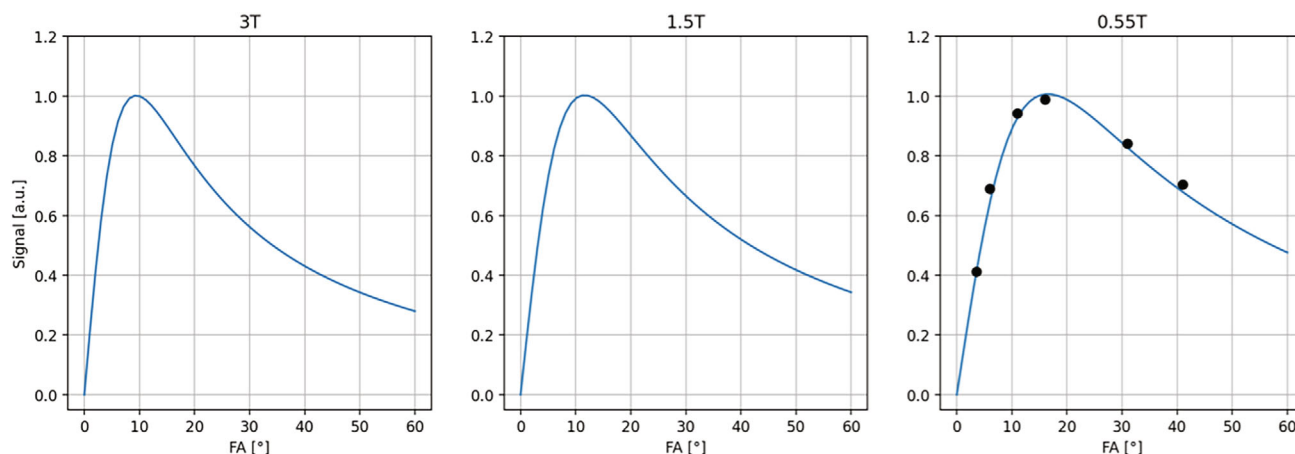


FIGURE 1 FA optimization at 0.55T, as compared to high-field systems. Experiment (dots) match simulation (lines) and reflect an optimal FA of approximately 15° for fat. The experimental values were calculated by taking the mean signal in fat divided by the standard deviation in a background region of interest. Simulation parameters were $T_1 = 370/290/190$ ms and $TR = 5/6/8$ ms for 3T/1.5T/0.55T (different TR were used for different field strengths since higher field strengths normally allows for shorter TR).

of those. Note that CV_w values may inflate when the mean is low, such as for MFI and liver PDFF.

3 | RESULTS

Figure 1 illustrates the dependence of lipid signal on FA for SPGR at different field strengths. For 0.55T, the variable FA experiment (dots) and simulation (lines) match closely and indicate an optimal FA of 15° for fat-referenced MRI. This is higher than the 10° that is typically used at 1.5 and 3T, as expected, because of the shorter T_1 . Other imaging parameters were optimized in a similar fashion, by performing parameters sweeps. Key imaging parameters: field of view = 500×405 mm², slice thickness = 5 mm, average = 1, bandwidth = 250 Hz/Px, no parallel imaging, bipolar readout gradient, weak asymmetric echo, 2D distortion correction, $TE_1 = 2.45$ – 2.54 ms or minimum TE allowed, $TE_2 = 6.47$ ms or opposed phase TE, $TR = 9.48$ – 9.53 ms or minimum allowed. The final 10-min protocol is summarized in Tables 1 and S1.

Figure 2 and Video S1 illustrates one representative male result, and Figure 3 and Video S2 illustrates one representative female result. Both show calibrated fat and water images in a coronal view, with color-coded segmentations of VAT, ASAT, and thigh muscle groups.

Image quality and repeatability were assessed in all 10 subjects (5 M/5F, age 25–60, body mass index [BMI] 20–30) with no scan failures. Counting all measurements in all 20 scans yields a theoretical maximum of 280 measurements in the study. A total of two minor and seven major signal issues were identified by the quality control, resulting in 273 produced measurements (97.5% analyzable). The two minor issues were complex fat/water swap in ASAT in the

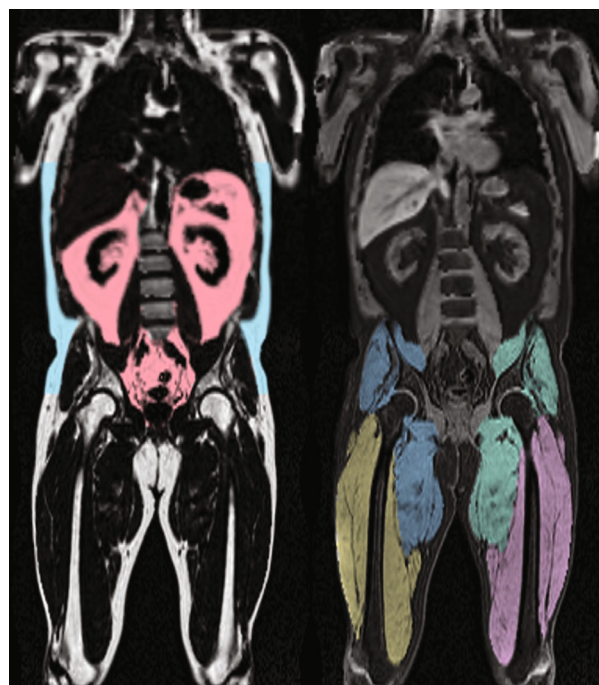


FIGURE 2 The 0.55T body composition profiling from one representative male subject (male, 57 y old, body mass index 29), 500 mm FOV in the left–right direction. Notice the clean fat-water separation with no obvious swaps. Adequate SNR is achieved for segmentation and visualization of all relevant structures. Note the good performance of automated segmentation. One mid-coronal slice is shown here. A movie that pans through all coronal slices is included in Video S1.

two scans of one subject. The major issues consisted of one breath hold technique issue affecting VAT, one calibration issue affecting ASAT, one global fat/water swap in liver PDFF (6p), and four acceleration artifacts in the MEGRE

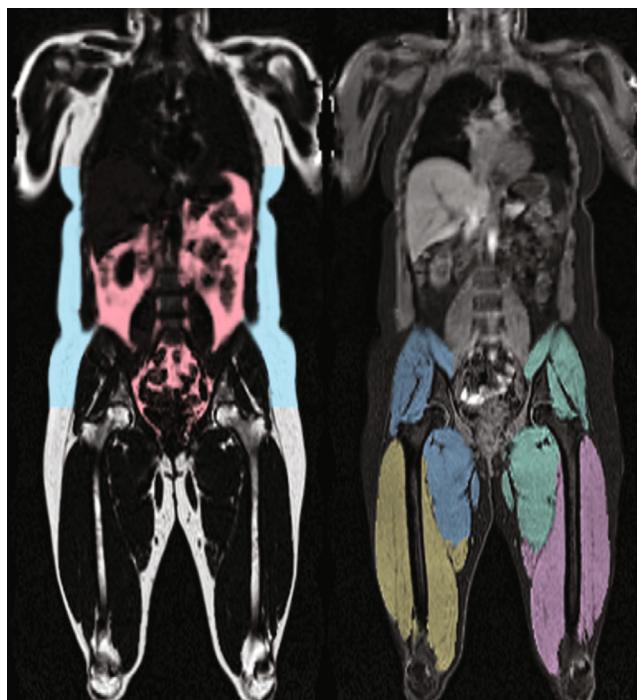


FIGURE 3 The 0.55T body composition profiling from one representative female subject (female, 28 y old, BMI 29), 500 mm FOV in the left–right direction. Notice the clean fat-water separation with no obvious swaps. Notice the adequate SNR for segmentation and visualization of all relevant structures. Notice the good performance of automated segmentation. One mid-coronal slice is shown here. A movie that pans through all coronal slices is included in Video S2.

used for liver T2* quantification affecting test and retest of liver PDFF (2p) for two subjects. This acceleration artifact was identified early in the study and was resolved by lowering the acceleration factor. The overall success rate (97.5%) is comparable to prior studies.¹⁵

Table 2 shows descriptive statistics in terms of mean and standard deviation of body composition metrics over the cohort, along with the repeatability results including number of observations available for the test–retest analysis.

4 | DISCUSSION

Body composition imaging at 0.55T is feasible with short scan times (<10 min) and has the potential to be another strong application for low-field and mid-field MRI. The low cost, footprint, and wide bore of new commercial low-field scanners are all characteristics in favor of body composition imaging and population screening.

SNR was not a major limitation in this study. This is in large part due to the fact that MRI body composition profiling is not a signal starved technique, evidenced by the fact that integrated body RF coil reception is typically used at conventional field strengths. The SNR at 0.55T was adequate and comparable to what is commonly observed at 1.5T due to the shorter T1 and lower readout bandwidth. In this study, we had no major challenges achieving equivalent voxel resolution to what is recommended at 1.5T. We observed some water-fat swaps in the arms, which are at

TABLE 2 Descriptive statistics of the study cohort and test–retest repeatability of 0.55T body composition profiling

Measurement	Mean	SD	N	s_w	RC	CV_w
VAT (cL)	304.44	209.71	10	4.25	11.79	2.22%
ASAT (cL)	713.74	345.16	10	16.93	46.94	1.94%
Total thigh volume (cL)	1236.41	279.16	10	5.25	14.56	0.46%
Left anterior thigh volume (cL)	223.34	52.14	10	2.30	6.38	0.90%
Right anterior thigh volume (cL)	227.42	59.43	10	2.07	5.74	0.87%
Left posterior thigh volume (cL)	392.86	84.27	10	2.26	6.27	0.60%
Right posterior thigh volume (cL)	392.79	86.75	10	2.13	5.89	0.69%
Mean anterior thigh MFI (pp)	5.62	0.96	10	0.10	0.29	2.03%
Left anterior thigh MFI (pp)	5.64	0.87	10	0.15	0.41	3.06%
Right anterior thigh MFI (pp)	5.60	1.06	10	0.09	0.25	1.60%
Left posterior thigh MFI (pp)	7.99	1.62	10	0.15	0.42	2.25%
Right posterior thigh MFI (pp)	7.99	1.63	10	0.12	0.32	1.57%
Liver PDFF (6p) (pp)	4.58	3.08	10	0.15	0.41	3.26%
Liver PDFF (2p) (pp)	3.08	2.21	8	0.17	0.47	6.72%

Abbreviation: RC, repeatability coefficient.

the edge of the FOV. We believe this artifact was due to gradient nonlinearity that is most significant towards the edge of the bore. Since arms are excluded in body composition profile analysis, this artifact did not affect the quantitative results.

It is important to carefully select imaging parameters for each new field strength. We found that the first TE and the echo spacing are especially important to select carefully. At lower field strengths, it is time-efficient to use the first echo as the approximate “in-phase” echo. And the second echo is best placed close to an out-of-phase time. Because the echo spacing is longer, it is beneficial to use a lower readout bandwidth which also improves SNR. At lower field strengths, the optimal FA is higher (Figure 1) primarily due to the shortening of lipid T1 and the longer minimum TR, because of the larger echo spacing.

The protocol was successfully optimized as demonstrated by the robust outcomes in terms of zero scan fails, good image quality and only nine quality issues among 280 measurements. The test-retest results further indicated that body composition analysis is viable and reliable at 0.55T, with a repeatability comparable to that of higher field strengths.³ Future work is needed to assess between-scanner reproducibility, and reproducibility against other field strengths.

Liver fat fractions were all small in the study cohort. As a result, the accuracy of PDFF in people with hepatic steatosis should be further confirmed with the current protocol in subjects with a broad range of PDFF. Furthermore, this study did not include a systematic investigation into the optimal protocol for multi-echo liver PDFF quantification at 0.55T. We hope to address these questions in future work.

This study was performed on a “ramped down” 0.55T system with high performance gradients and a 70 cm bore. The proposed protocol may require adjustments to run on new commercial 0.55T MRI systems that have weaker gradients, but also provide a wider 80 cm bore. Weaker gradients are expected to increase the minimum achievable echo-time. The 80 cm bore may overcome or at least alleviate three currently insurmountable challenges when using MRI body composition profiling in bariatric and obese patient populations on conventional 60/70 cm bore scanners: (1) these patient populations are often contraindicated to MRI owing to the patient’s physical size; (2) the body habitus is often outside of the imaged field of view, rendering the missing anatomy unquantifiable; and (3) the image quality at the periphery of the imaged field of view is often distorted and measurable anatomy rendered unanalyzable. A feasibility and precision study in an obese population is needed to elucidate the value of low field wide bore MRI as a tool in body composition profiling in obese and bariatric patient populations.

5 | CONCLUSIONS

The 0.55T body composition MRI protocol was successfully implemented and optimized. The resulting MR images yield satisfactory quality for automated post-processing and body composition analysis was found to be robust and repeatable.


ACKNOWLEDGMENTS

We acknowledge grant support from the National Science Foundation (No. 1828736), and research support from Siemens Healthineers and AMRA Medical. MRI scan time was provided by the USC Dynamic Imaging Science Center. We thank Mary Yung for research coordination.

CONFLICT OF INTEREST STATEMENT

S.X. Cui and X. Zhong are employees of Siemens. S. Weston and A. Ahlgren are employees of AMRA Medical.

ORCID

Krishna S. Nayak  <https://orcid.org/0000-0001-5735-3550>

Sophia X. Cui  <https://orcid.org/0000-0002-5133-4903>

Xiaodong Zhong  <https://orcid.org/0000-0001-8355-5279>

REFERENCES

- Linge J, Borga M, West J, et al. Body composition profiling in the UK biobank imaging study. *Obesity*. 2018;26:1785-1795.
- Tejani S, McCoy C, Ayers CR, et al. Cardiometabolic health outcomes associated with discordant visceral and liver fat phenotypes: insights from the Dallas heart study and UK biobank. *Mayo Clin Proc*. 2021;97:225-237.
- Borga M, Ahlgren A, Romu T, Widholm P, Dahlqvist Leinhard O, West J. Reproducibility and repeatability of MRI-based body composition analysis. *Magn Reson Med*. 2020;84:3146-3156.
- Dixon WT. Simple proton spectroscopic imaging. *Radiology*. 1984;153:189-194.
- Hu H, Nayak K. Quantification of absolute fat mass using an adipose tissue reference signal model. *J Magn Reson Imaging*. 2008;28:1483-1491.
- Leinhard OD, Johansson A, Rydell J, et al. Quantitative abdominal fat estimation using MRI. *Proceeding of the 19th international conference on pattern recognition*. IEEE; 2008: 2137-2140.
- Yokoo T, Serai SD, Pirasteh A, et al. Linearity, bias, and precision of hepatic proton density fat fraction measurements by using MR imaging: a meta-analysis. *Radiology*. 2018;286: 486-498.
- Marques JP, Simonis FFJ, Webb AG. Low-field MRI: an MR physics perspective. *J Magn Reson Imaging*. 2019;49:1528-1542.
- Wald LL, McDaniel PC, Witzel T, Stockmann JP, Cooley CZ. Low-cost and portable MRI. *J Magn Reson Imaging*. 2020;52:686-696.
- Campbell-Washburn AE, Ramasawmy R, Restivo MC, et al. Opportunities in interventional and diagnostic imaging by

using high-performance low-field-strength MRI. *Radiology*. 2019;293:384-393.

11. Bernstein MA, Zhou XJ, Polzin JA, et al. Concomitant gradient terms in phase contrast MR: analysis and correction. *Magn Reson Med*. 1998;39:300-308.
12. Lee NG, Ramasawmy R, Lim Y, Campbell-washburn AE, Nayak KS. MaxGIRF: image reconstruction incorporating Maxwell fields and gradient impulse response function distortion. *Magn Reson Med*. 2022;88:691-710.
13. Pineda A, Reeder S, Wen Z, Pelc N. Cramér-Rao bounds for three-point decomposition of water and fat. *Magn Reson Med*. 2005;54:625-635.
14. Zhong X, Nickel MD, Kannengiesser SA, Dale BM, Kiefer B, Bashir MR. Liver fat quantification using a multi-step adaptive fitting approach with multi-echo GRE imaging. *Magn Reson Med*. 2014;72:1353-1365.
15. West J, Leinhard OD, Romu T, et al. Feasibility of MR-based body composition analysis in large scale population studies. *PLoS One*. 2016;11:e0163332.

SUPPORTING INFORMATION

Additional supporting information may be found in the online version of the article at the publisher's website.

Table S1: Full details of the optimized MRI protocol for 0.55 T body composition profiling (Siemens “ramped

down” 0.55 T Aera XQ). Abbreviated parameters are listed in Table 1.

Video S1: 0.55 T body composition profiling from one representative male subject (Male, 57 year old, BMI 29), with mid-coronal slice shown in Figure 2. Notice the clean fat-water separation with no obvious swaps. Notice the adequate SNR for segmentation and visualization of all relevant structures. Notice the good performance of automated segmentation.

Video S2: 0.55 T body composition profiling from one representative female subject (Female, 28 year old, BMI 29), with mid-coronal slice shown in Figure 3. Notice the clean fat-water separation with no obvious swaps. Notice the adequate SNR for segmentation and visualization of all relevant structures. Notice the good performance of automated segmentation.

How to cite this article: Nayak KS, Cui SX, Tasdelen B, et al. Body composition profiling at 0.55T: Feasibility and precision. *Magn Reson Med*. 2023;90:1114-1120. doi: 10.1002/mrm.29682